CORROSION SCIENCE AND TECHNOLOGY, Vol.2, No.1(2003), pp.41~46

Electrochemical Analysis on Flow-Accelerated Corrosion Behavior of SA106 Gr.C Steel in Alkaline Solution

Jun Hwan Kim, In Sup Kim, and Han Sub Chung*

Department of Nuclear Engineering, Korea Advanced Institute of Science and Technology
373-1 Kusong-dong, Yusong-gu, Taejon, Korea, 305-701
**Korea Electric Power Research Institute, 103-16, Munji-ding*
Yusong-gu, Taejon, Korea, 305-380

Flow-Accelerated Corrosion behavior concerning both activation and mass transfer process of SA106 Gr.C steel was studied using rotating cylinder electrode in room temperature alkaline solution by DC and AC electrochemical techniques. Passive film was formed from pH 9.8 by step oxidation of ferrous product into hydroxyl compound. Corrosion potential shifted slightly upward with rotating velocity through the diffusion of cathodic species. Corrosion current density increased with rotating velocity in pH 6.98, while it soon saturated from 1000 rpm at above pH 9.8. On the other hand the limiting current increased with rotating speed regardless of pH values. It seems that activation process, which represents formation of passive film on the bare metal surface, controls the entire corrosion kinetics

Keywords : *flow-accelerated corrosion, alkaline solution, rotating cylinder electrode, activation, mass transfer*

1. Introduction

Nowadays, more and more piping systems in power plant suffer from problems related to the Flow-Accelerated Corrosion (FAC). FAC is a process where the protective oxide layer on carbon or low-alloy steel dissolves into a stream of flowing water or a water-steam mixture. Stable but faster corrosion rate is maintained where the dissolution rates of ferrous ions by the activation and the removal rates caused by concentration-driven mass transfer are equal. Eventually, a thinned component would fail due to overstress from operating pressure or abrupt changes in conditions such as waterhammer, start-up loading, and so on. It first appeared in a nuclear power plant by the condensate system failure in Surry, which resulted in several casualties. Thus it is now considered as one of the main degradation mechanisms on secondary piping in PWR, along with high cycle fatigue.[1),2)] Whereas FAC problems in CANDU primary heat transport system did not emerge because its water chemistry seemed to be far from corrosion until the Point Lepreau feeder leak accident happened in late 1996. After AECL's recommendation of periodic monitoring feeder wall thickness, most of the CANDU-6 plant, such as Gentilly-2, Embalse, Pickering, and Wolsong, reported the same problem related to FAC.[3)] And it is recognized as potential hazard in CANDU primary heat transport system because corrosion parameters are not fully investigated in simulated CANDU environments, not to mention of clarifying FAC mechanisms and proposing mitigation strategies in operating power plant.

The purposes in this study are to observe FAC behavior of low alloy piping steel in simulated CANDU primary coolant condition using rotating cylinder electrode, and to propose electrochemical methodology in analyzing velocity sensitivity regarding the kinetics of activation and mass transfer behavior which constitute the entire FAC process.

2. Experimental procedures

2.1 Test condition and corrosion experiment

Water chemistry in this study was simulated after the CANDU primary water coolant conditions. Thus experimental solution was composed of distilled water and lithium hydroxide (LiOH). All the solutions in this study were de-aerated by nitrogen gas injection for 3 hours and pH of the solution was selected as 9.84, 10.6, and 11.83 by the step titration with 1M LiOH. When testing in neutral solution, 300 ppm boric acid and weak LiOH were introduced at the value of pH 6.96[4)] to raise conductivity

but avoid severe deviation of water chemistry, such as appearance of unintended passivation which seldom appears in the neutral solutions. Test material in this study is SA106 Gr.C steel with similar chromium content and microstructure to SA106 Gr.B steel which is used as the feeder materials.[5]

Polarization test was conducted through the three-electrode system using scanning potentiostat to observe electrochemical parameters. The reference electrode and auxiliary electrode were saturated calomel electrode (SCE) and graphite, respectively. Scan rate was 0.5 mV/sec. Corrosion current density was measured through both Tafel extrapolation and linear polarization method near the corrosion potential. Electrochemical impedance spectroscopy test was performed in order to analyze charge transfer reaction of the low alloy steel in alkaline solution. Applied frequency was decreased successively from 1 MHz to 100 μHz with each voltage amplitude is 0.2 mV to maintain linearity between input and output signal. Test conditions of the AC method are identical to the DC method.

2.2 Rotating cylinder electrode (RCE) experiment

Fig. 1 shows a schematic diagram of RCE setup. Spring-pushed bridge was contacted to rotating bar for the extraction of electric signal and application of external potential into working electrode. A bypass circuit between reference and working electrode has been installed to investigate if contact resistance and related thermal resistance between the bridge and rotating bar can affect the total current in given RCE system. Result of potential value at each junction point can be shown that potential which exerts driving force of overall corrosion process and potential which represents open-circuit potential are almost equal during the test period. To diminish IR drop variation during the entire test period, a reference electrode was inserted in an inclined position and fixed as close as possible to maintain constant distance between electrodes. Baffles were attached in upper part of RCE cell to avoid generation of Taylor vortices and observe pure single phase flow effect. All specimens were ground with emery paper, and finally polished down to the 6 μm grit in which effect of surface roughness assumed to be negligible as the concentration boundary layer thickness of the rotating fluid, After grinding, they were de-greased by acetone and charged in -1,000 mV (SCE) to remove oxide on the specimen prior to the experiment. The working electrode was taken parallel to the orientation along which the coolant actually flowed, as implied in Fig. 2. Corrosion potential in this study was decided at the point where anodic half-cell current (i_a) and cathodic half-cell current

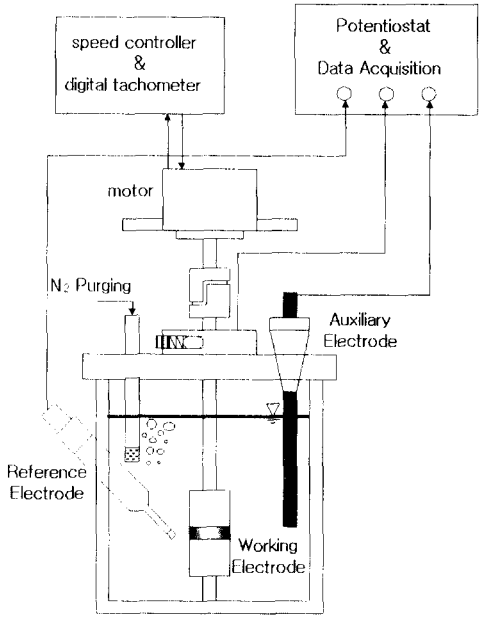

Fig. 1. Schematic illustration of RCE setups

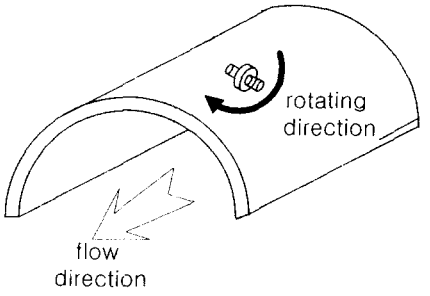

Fig. 2. Metallographic orientation of RCE specimen

(i_c) are equal. Corrosion current was measured by aforementioned method.

3. Results and discussions

3.1 Effect of pH on the corrosion process in alkaline solution

Fig. 3 shows potentiodynamic result with increasing pH. Metal simply dissolves in the anodic potential regime at neutral condition, showing no passive film formation on the surface. Meanwhile, it was formed in an incomplete manner from pH 9.84. Above pH 10.4, the film appeared stable from the observation of the passivation potential and the average film current density. Fig. 4 shows polarization curve magnified in active-passive regime with increasing alkalinity. As seen from this figure, two characterized peaks appeared at each active-passive transition potential. Similar results were reported by Zhou who

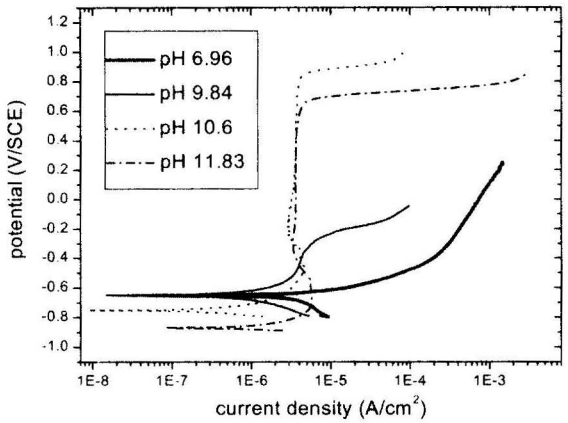

Fig. 3. Electrochemical results of SA106 Gr.C steel in static condition

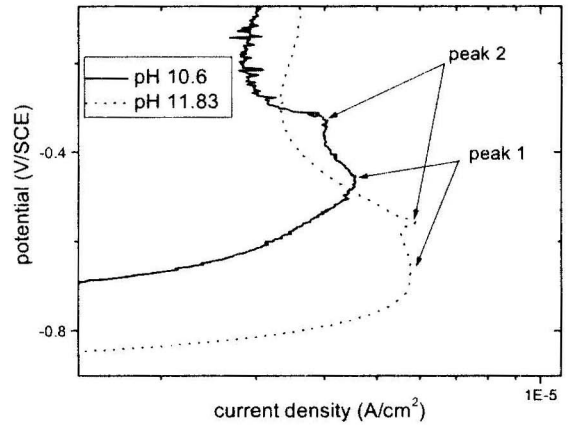

Fig. 4. Magnified section at active-passive transition regime of polarization curve in alkaline solution

studied corrosion behavior of mild steel at concentrated NaOH solutions.[6] He proposed that first anodic peak combined three parallel processes, which were composed of active dissolution of iron to a soluble bi-valent ion product of $HFeO_2^-$, formation of a surface layer and passive film, and formation of a soluble tri-valent iron species of FeO_2^- prior to the onset of passivation, and second anodic process represented the oxidation of the Fe_3O_4 magnetite film to Fe_2O_3, FeO_2^-. Proposed electrode reactions at each anodic potential based on our experimental results are as follows;[7),8)]

First peak : E(vs. SHE) = 0.925 − 0.114pH

$$3Fe(OH)_2 + 2OH^- \rightarrow Fe_3O_4 + 4H_2O + 2e^- \quad (1)$$

$$E = -0.114 - 0.059pH$$

$$Fe(OH)_2 + 2OH^- \rightarrow FeO_2^- + 2H_2O + e^- \quad (2)$$

$$E = 0.786 + 0.059\log[FeO_2^-] - 0.118pH$$

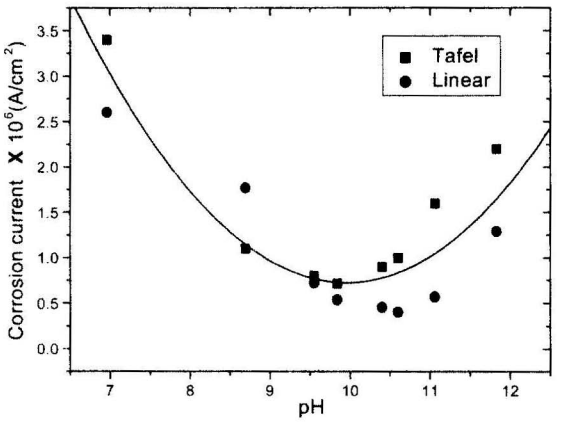

Fig. 5. Results of Tafel and linear polarization with pH difference in static condition

Second peak : E(vs. SHE) = 1.387 − 0.142pH

$$Fe_3O_4 + H_2 + 2OH^- \rightarrow 3(\gamma - FeOOH) + H^+ + 3e^- \quad (3)$$

$$E = 1.916 - 0.019\log P_{H2} - 0.059pH$$

$$Fe_3O_4 + 4OH^- \rightarrow 3FeO_2^- + 2H_2O + e^- \quad (4)$$

$$E = 2.411 + 0.177\log[FeO_2^-] - 0.236pH$$

Fig. 5 shows the plot of corrosion current density calculated both by Tafel and linear polarization with pH. In this figure, they behave more or less of parabolic shapes with the local minima at pH 10.4. This seems to be inconsistent with the conventional weight loss data of mild steel in high pH solutions.[9] Such an increasing tendency of corrosion current density above pH 10.4 can be explained by the electrochemical nature of alkaline corrosion,[10] which governed the kinetic reaction of iron electrode like;

Anodic half-cell reaction : $Fe + 2OH^- \rightarrow Fe(OH)_2 + 2e^-$ (5)

$$i_a = 2k_a F[OH^-]^{1.5} \exp\{FE/RT\} \quad (6)$$

Cathodic half-cell reaction : $H_2O + e^- \rightarrow \frac{1}{2}H_2 + OH^-$ (7)

$$i_c = -k_c F[H_2O] \exp\{-FE/2RT\} \quad (8)$$

Where k_a and k_c denote anodic and cathodic reaction rate constant. In case of increasing hydroxyl ion concentration, each anodic and cathodic half-cell current density increases such that entire corrosion exchange current density increases on the bare metal surface near the corrosion potential, in which both anodic and cathodic reaction may compete. When the passive film is formed, such a current transient will drop to a stable value, which causes suppressing metal loss. Fig. 6 is the impedance test result of the low alloy steel in the open circuit potential

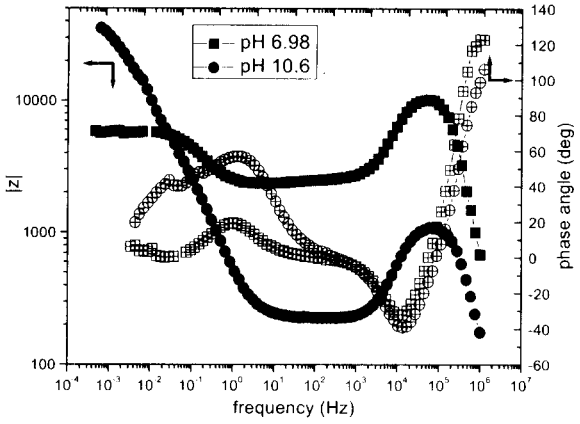

Fig. 6. Bode plot of low alloy steel in alkaline solution

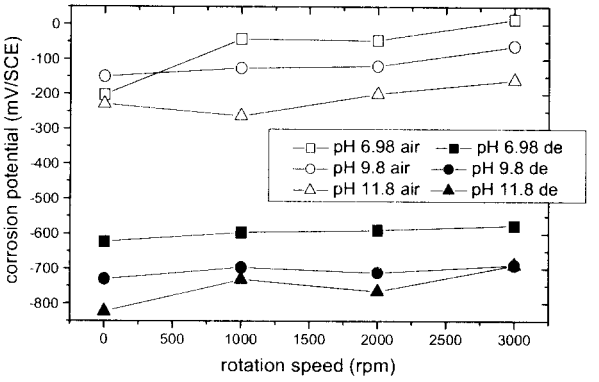

Fig. 8. Electrochemical corrosion potential with rotating speed and oxygen content

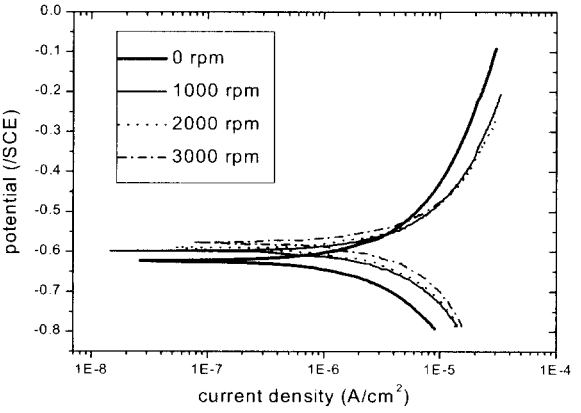

Fig. 7. Results of RCE in neutral solution

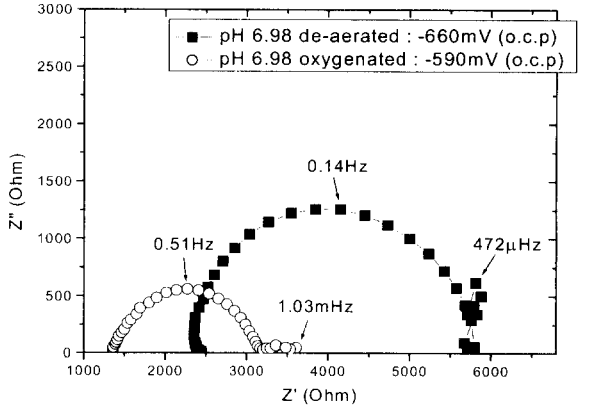

Fig. 9. Nyquist plot of low alloy steel with oxygen contents

with pH variation. The resistance, which takes part in the activation-related charge transfer reaction, greatly increased with pH value. On the other hand, pseudo-capacitance and inductance appeared at the high and intermediate frequency were soon eliminated at below 0.19Hz in neutral solution and at below 1.38Hz in pH 10.6 in which actual charge transfer reaction took place.

3.2 Effect of rotation speed on the corrosion process

Fig. 7 is the polarization curve versus rotating velocity in neutral solution. It was observed that both the corrosion potential and the dissolution current density at anodic regime augment with rotating velocity. The upward shift of corrosion potential with rotating velocity may be due to the migration of reducing agent to the metal electrode more easily with turbulent flow.[11] Fig. 8 is the plot of corrosion potential with rotating speed and addition of dissolved oxygen species. Potential rises significantly with addition of oxygen. Also, the corrosion potential escalated at the similar rate regardless of oxygen contents with rotating speed, it indicates that although cathodic reaction soon switched from oxygen reduction to reduction of water molecule with deprivation of dissolved oxygen, the transport kinetics both of the oxidizing agents would totally be dependent on mechanisms of diffusion. Increment of rotating speed results in narrowing the diffusion concentration boundary layer, causes the accelerated transfer of oxidizing agent to the metal surface. Such postulate was also depicted in AC behavior, as implies in fig 9. At low frequency regime in oxygenated condition, retarding behavior on the charge transfer process appeared, which resulted from the diffusion process of oxygen molecules at low frequency. The same kind of stagnation appeared in deoxygenated condition which is evident from the fact that although oxidation of the ferrous ion plays a role in the reaction, diffusion of the reactant caused by cathodic reaction, such as hydrogen also intervenes more or less in the entire corrosion process .[12]

3.3 Electrochemical analysis between activation and mass transfer process

Fig. 10 is the result of corrosion current density with different pH and rotating velocities in single phase flow condition. It more or less increased with rotating velocity in neutral condition. On the other hand, it soon saturated with velocity above pH 9.8. It seems that there exists a process controlling the entire corrosion kinetics regardless of rotating velocity in alkaline condition. Such a result may be compared with that of Denpo who measured corrosion rate of carbon steel and 13% chromium alloy in 2% NaCl solution containing CO_2.[13] He reported that carbon steel, on which passive film did not form, showed a great increase of corrosion rate with rotating speed, whereas 13% Cr steel, in which passive film was apt to generate in open circuit potential, showed saturation of corrosion rate above 1000 rpm. Fig. 6 indicates that capacitance component in pH 10.6 increased ten times as compared with in neutral solution. The result may coincide

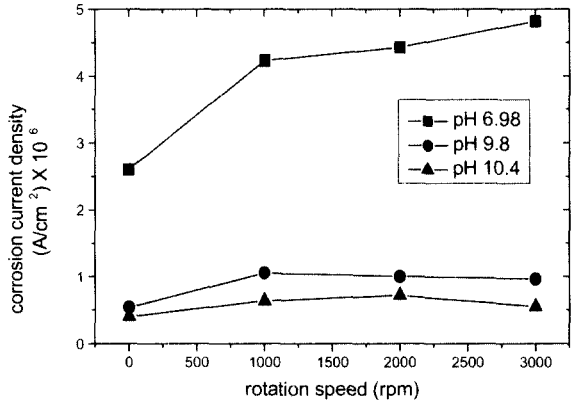

Fig. 10. Results of linear polarization with pH difference

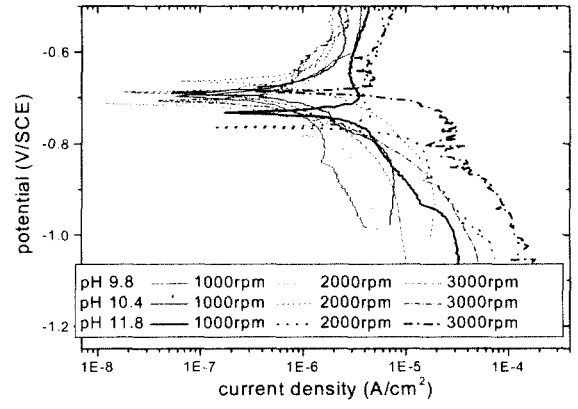

Fig. 11. Cathodic branch of polarization curve in different pH and rotating velocities

with the hypothesis that formation of passive film, which acts as insensitive component to the fluid velocity, takes a large portion of entire activation process with increase of pH. The increasing tendency of charge transfer process at bare metal, sensitive of corrosion rate with fluid will be dominant in activation-controlled corrosion system.

Limiting current density was measured in cathodic branch to investigate which parameters have a main influence on the entire corrosion process with rotating velocity. Fig. 11 is the result of limiting current density with pH and rotating velocity, shows sensitive change with rotating velocity. Suppose that the governing reaction at cathodic branch relies on the diffusion process of reducing species rather than the charge transfer activation process, the whole reaction kinetics of FAC in room temperature alkaline solution can be confined by the activation process which represents formation of the passive film on the bare metal surface. It can be associated with the fact that cathodic current responds as more or less retarding asymptotic behavior with applied potential compared to the polarization curve dominated in the pure mass transfer, which can be deduced that entire corrosion mechanism is governed by the mixed reaction of the activation and mass transfer.[14] This is consistent with the assumption of the previous FAC model, where it defines that activation process on the steel surface can govern the rate-determining step by the flow velocity to a certain extent.[15]

4. Conclusions

1) Corrosion current density decreased up to pH 10.4 but it soon increased with pH, which is due to the tendency of alkaline corrosion with increase of each half-cell current controlled by individual reacting concentrations.

2) Corrosion potential slightly increased with rotating velocity, which could be associated with the enhanced diffusion of molecular oxidizing agent.

3) Corrosion current density increased with rotating velocity in neutral solution, whereas it soon saturated from 1000 rpm above pH 9.8, That indicates that the activation process, which represents the formation of passive film on bare metal surface based on the mechanisms like piecewise transformation of ferrous species into hydroxyl compounds, rather than mass transfer process, confines the entire corrosion process in alkaline condition.

Acknowledgement

This work was partially supported by the Korea Electric Power Research Institute and by the Brain Korea 21 project from the Korean Ministry of Education & Human

Resources Development.

References

1. W. J. Shack, Proc. of the 3rd International Symposium on Environmental Degradation of Materials in Nuclear Power Systems - Water Reactors 55 (1988).
2. V. Shah, and P. E. Macdonald, Aging and Life Extension of Major Light Water Reactor Components 523 (1993).
3. K. A. Burill, and E. L. Cheluget, "Corrosion of CANDU Outlet Feeder Pipes", JAIF Int'l Conf. On Water Chemistry 699 (1998).
4. J. H. Kim and I. S. Kim, "Environmentally Assisted Crack Growth Behavior of SA508 Cl.3 Pressure Vessel Steel", Proc. of the KNS Spring Meeting, 154 (1998).
5. KINS REPORT, No. 756.05
6. J. Y. Zou, and D. T. Chin, "Anodic Behavior of Carbon Steel in Concentrated NaOH Solutions", *Electrochimica Acta*, **33**(4), 477 (1988).
7. J. Y. Zou, and D. T. Chin, "Mechanism of Steel Corrosion in Concentrated NaOH Solutions", *Electrochimca Acta*, **32**(12), 1751 (1987).
8. T. Misawa, "The Thermodynamic Consideration for Fe-H_2O System at 25 ℃", *Corr. Sci.*, **13**, 659 (1973).
9. D. A. JONES, Principles and prevention of Corrosion 357 (1992).
10. G. Bellanger, "Effect of carbonate in slightly alkaline medium on the corrosion of maraging steel", *J. of Nucl. Mat.*, **217**, 187 (1994).
11. Y. J. Kim, C. C. Lin, and R. Phathania, "Electrochemical Corrosion Potential Measurement with a Rotating Cylinder Electrode in 288 ℃ Water", Proc. Of the Water Chemistry of Nuclear Reactors System 6, BNES p.139 (1992).
12. J. G. Kim, "A Study on the Flow-Accelerated Corrosion Characteristics of Galvanically Coupled Dissimilar Metals", 1st Workshop on the Evaluation of Pipe Wall Thinning in Nuclear Power Plants, KINS/PR-012 (2000)
13. K. Denpo and H. Ogawa, "Fluid Flow Effects on CO_2 Corrosion Resistance of Oil Well Materials", *Corrosion*, **49**(6), 442 (1993).
14. S. W. Dean, "Velocity-Accelerated Corrosion Testing and Predictions", *Material Protection*, Sept p.61 (1990).
15. B. Chexal, "Flow-Accelerated Corrosion in Power Plan t", EPRI report TR-106611, pp.4-33 (1996).